Applied Radiation and Isotopes 83 (2014) 196–199

Contents lists available at ScienceDirect

Applied Radiation and Isotopes

journal homepage: www.elsevier.com/locate/apradiso

Thermoluminescent characterization of HfO_2:Tb^{3+} synthesized by hydrothermal route

E. Montes [a], P. Cerón [a], T. Rivera Montalvo [a,*], J. Guzmán [a], M. García-Hipólito [b], A.B. Soto-Guzmán [c], R. García-Salcedo [a], C. Falcony [c]

[a] Centro de Investigación de Ciencia Aplicada y Tecnología Avanzada, IPN, Unidad Legaria, Avenida Legaria 694 Colonia Irrigación, 11500 México D.F., México
[b] Instituto de Investigaciones en Materiales, UNAM, Circuito Exterior, Ciudad Universitaria, Coyoacán, 04510 México D.F., México
[c] Departamento de Física, CINVESTAV, IPN, Apartado Postal 14-740, 07000 México D.F., México

HIGHLIGHTS

- Thermo and photoluminescent properties of nanoparticles (NPs) of hafnium oxide (HfO_2), both intrinsic and doped with terbium (Tb^{3+}) were analyzed.
- Nanoparticles of HfO_2:Tb^{3+} were grown by hydrothermal route.
- Thermoluminescence of HfO_2:Tb^{3+} nanoparticles suggests good candidate as UVR dosimeter.
- Thermoluminescence of HfO_2:Tb^{3+} suggests shallow traps as luminescent center.

ARTICLE INFO

Available online 10 July 2013

Keywords:
HfO_2:Tb
Hydrothermal
Thermoluminescence
Photoluminescence

ABSTRACT

Thermo and photoluminescent properties of nanoparticles (NPs) of hafnium oxide (HfO_2), both intrinsic and doped with terbium (Tb^{3+}) are reported. The NPs of HfO_2 were synthesized by hydrothermal route, using hafnium tetrachloride ($HfCl_4$) and terbium chloride hexahydrated ($TbCl_3{\bullet}6H_2O$) as precursors and sodium hydroxide (NaOH) to adjust the pH. Deionized water was used as solvent in all cases. The synthesis was carried out at different dopant concentrations from 0 to 20 at% of terbium with respect to the amount of hafnium in the precursor solution. The temperature of hydrothermal treatment was 200 °C and 80 min of reaction time. X-ray diffraction results show that at terbium concentrations higher than 15 at% the HfO_2 nanoparticles have a crystalline structure corresponding to the tetragonal phase. Thermoluminescent (TL) characterization was performed after 5 min irradiation of the samples with ultraviolet light of 200 nm wavelength. The highest TL emission was observed on samples with 7 at% of Tb, with the TL peak centered at 128 °C. Thermoluminescence analysis shows behavior associated with second-order kinetics with activation energy of 0.49 eV. Photoluminescent spectrum present the characteristics $^5D_4 \rightarrow {}^7FJ$ ($J=3$–6) terbium ion electronic transitions lines centered on 489 nm, 543 nm, 584 nm and 622 nm.

1. Introduction

In recent decades, the measurement of ultraviolet radiation (UVR) has been of great interest, because overexposure to this kind of radiation can cause undesirable biological effects in the human beings (Trüeb and Tobin, 2010). In natural environment, the Sun's UVR has significant effects on all living beings. However, few studies exist related with real effect of these radiations (Guzmán-Mendoza et al., 2010). In addition, little work has been done to produce new materials for UVR personal and environmental dosimetry (Rivera Montalvo et al., 2005). In recent years, the hafnium oxide has been studied for its possible applications as scintillators, CO_2 detectors and dosimeters (Chacón-Roa et al., 2008; Lange et al., 2006). It's physicochemical properties, such as high melting temperature (2774 °C), high chemical stability, high crystallographic density (≈10 g/cm^3), low optical losses, hardness close to diamond in the tetragonal phase, as well as a wide optical band gap (5.68 eV) (García-Hipólito, 2002), make hafnium oxide (HfO_2) a material of interest for use as luminescent host lattice doped with rare earths (Mignotte, 2001). The transparency spectral range of HfO_2, which extends from the near ultraviolet to medium infrared (Yoshimura and Sōmiya, 1999), allows for the appearance of localized states (Villanueva-Ibañez et al., 2003), which

* Corresponding author. Tel.: +52 55 3660 8403.
E-mail address: trivera@ipn.mx (T. Rivera Montalvo).

0969-8043/$ - see front matter © 2013 Elsevier Ltd. All rights reserved.
http://dx.doi.org/10.1016/j.apradiso.2013.06.008

serve as traps that contribute to the thermoluminescent process. On the other hand, the rare earths are used as optical activators since they show narrow bands of emission and absorption, due to intra-configurational transitions *4f→4f*, with emissions peaked at well-defined wavelengths. Recent studies have shown that ion Tb^{3+} presents a more luminescent intensity, in relation to other trivalent ions of rare earths such as dopant. At present, there are various methods for obtaining nanostructured oxides, among which it is possible to mention sol–gel, co-precipitation, solvothermal, among others (LeLuyer et al., 2008). The hydrothermal method is one of the simplest and cheapest methods to perform the synthesis of metal oxides. It's use becomes necessary in the preparation of those oxides with high values of supersaturation that precipitate in amorphous structure (Meskin et al., 2007). Hydrothermal methodology allows to control size, morphology and the composition of the products of the reaction phase, in order to obtain homogeneous and dispersed nanoparticles, through the variation of parameters such as temperature, pressure, processing time, concentration and acidity (pH); The particle size control is the result of processes of coarsening and redissolution–recrystallization which take place under conditions of high pressure and temperature. This work reports the thermoluminescent and photoluminescence properties of hafnium oxide nanoparticles doped with terbium (HfO_2:Tb^{3+}) as a function of dopant concentration, obtained by the hydrothermal route.

2. Experimental details

The nanoparticles of HfO_2, intrinsic and doped with Tb^{3+}, were synthesized by the hydrothermal route (Byrappa and Adschiri, 2007; Štefanić et al., 2005; Yoshimura and Byrappa, 2008). An aqueous solution 0.02 M of $HfCl_4$ (Alfa Aesar 99%), in deionized water with the subsequently addition of $TbCl_3$•6H2O (Sigma Aldrich 99.9%) was prepared. The Tb^{3+}concentration were varied from 1 to 20 at%, with respect to the amount of hafnium in the precursor solution. The pH of the solution was adjusted to 12 by adding a 2 M NaOH solution drop by drop, under constant stirring for 15 min. 20 ml of the obtained suspension was placed into a Teflon vessel inside the stainless steel autoclave and subjected to hydrothermal treatment at 200 °C, under autogenously pressure at 80 min; after the autoclave was brought to room temperature, through a water cooling process. The resulting precipitate was repeatedly washed with deionised water, using a centrifuge to remove the excess of Cl^- and Na^+ ions. Finally the precipitate was dried at to room temperature for 24 h. The structural characteristics of the HfO_2 powders doped with Tb^{3+} ions were analyzed by X-ray diffraction (XRD) in a D8-Advance-Bruker diffractometer with wavelength radiation of 1.5406 Å (Cu Kα), at steps of 0.05° step and a 0.5 s per step. Energy Dispersive Spectroscopy (EDS) was used to obtain the elements present in the samples, by using an X-ray detector of silicon–lithium, Oxford model Pentafet. The IR measurements were carrying out using an infrared spectrophotometer with Fourier Transform (FT-IR), model Spectrum One by Perkin Elmer at room temperature. A pellet of the nanoparticles mixed with KBr as binder was used in all cases. The thermoluminescent (TL) spectrum was obtained with a TLD-3500-Harshaw reader. The photoluminescence (PL) spectra were obtained with a FluoroMax Horiba JobinYvon-P spectrofluorimeter, with a 150 W continuous emission xenon lamp. Scanning micrographs were obtained through a Field Emission Scanning Electron Microscope (FESEM) JOEL model JEM-7401F.

3. Results and discussion

Fig. 1 shows the XRD patterns for HfO_2:Tb^{3+} samples synthesized with a hydrothermal time of 80 min at 200 °C, as a function of Tb^{3+} concentration. At dopant concentrations below 15 at%, it is possible to observe an atomic structure mostly amorphous. While concentrations greater than 15 at%, diffraction peaks corresponding to the tetragonal phase of HfO_2 (reference JCPDS 08-0342) are present. At the highest Tb concentration the diffraction peaks become more defined and narrow, suggesting an increase in crystal size, and an overall improvement of crystallite quality in the HfO_2 particles, which may indicate that Tb^{3+} ions stabilize the crystalline phase of the HfO_2 particles (Villanueva-Ibañez et al., 2003).

Using the Scherrer's formula, it was possible to estimate the size of the crystallites (Cullity and Stock, 2001) from the half-width of the diffraction peak with Miller index (111). A crystal size of $\tau \approx 116$ Å was determined for the HfO_2 particles with 20 at% of Tb^{3+}.

Table 1 shows the Energy Dispersive Spectroscopy (EDS) measurements, of HfO_2 synthesized at different concentrations of terbium. The table shows a higher amount of oxygen than expected in the ideal stoichiometry of HfO_2 (33.0% Hf to 66.0% O), this could be associated with the complexes formed with the metals M–OH•nH_2O ($[Hf^{4+}]$•$[Tb^{3+}]$) in the amorphous phase.

Fig. 2 shows the infrared (IR) spectrum for intrinsic HfO_2, showing the characteristic absorption broad band of O–H at ~3400 cm^{-1}, which confirms the presence of water related bonds in these samples.

A FESEM image of the NP´s HfO_2:Tb^{3+} doped with 20 at% of terbium is shown in Fig. 3. It is possible to appreciate semi-spherical NP's, the particles appear considerably agglomerated, but

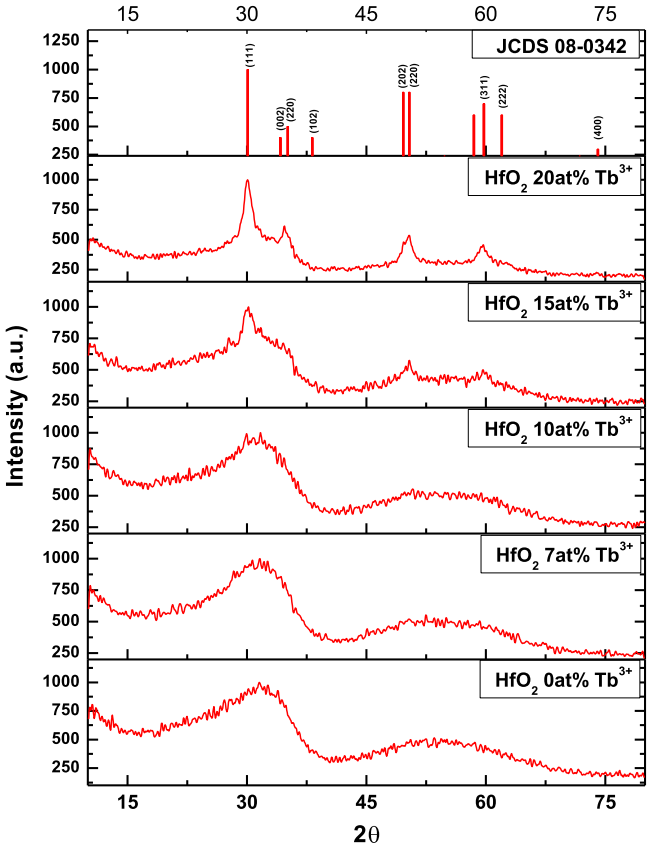

Fig. 1. Diffraction patterns of HfO_2:Tb^{3+}, synthesized by hydrothermal route, at different dopant concentrations.

Table 1
Atomic percent content in the hafnium oxide (HfO_2:Tb^{3+}) at different concentrations of dopant.

Concentration of Tb^{3+} (sol)	Atomic percent content (%)			
	Oxygen	Hafnium	Terbium	Tb^{3+}/Hf^{4+} (s)
0	79.47	20.56	**0.00**	**0.00**
1	78.12	21.88	**0.00**	**0.00**
3	77.38	22.22	0.40	1.80
5	78.24	20.58	1.18	5.73
7	77.72	20.76	1.52	7.32
10	79.95	18.18	1.87	10.29
15	78.24	19.03	2.73	14.35
20	77.52	18.89	3.59	19.00

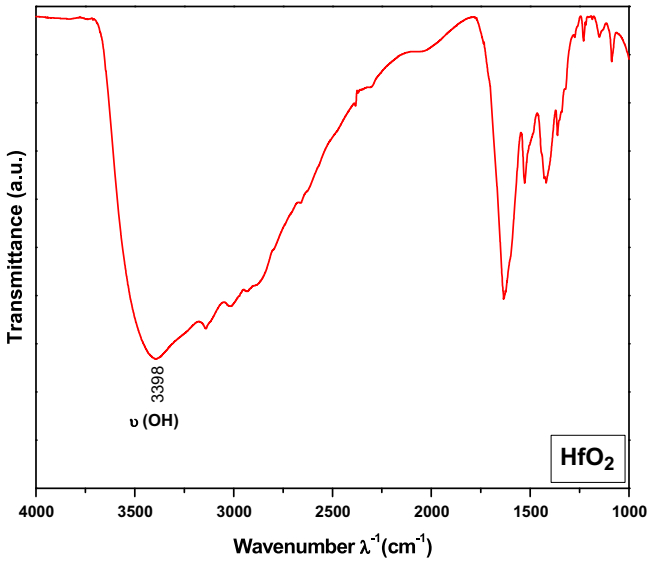

Fig. 2. IR spectrum for the intrinsic HfO_2 sample, the characteristic band for –OH is observed.

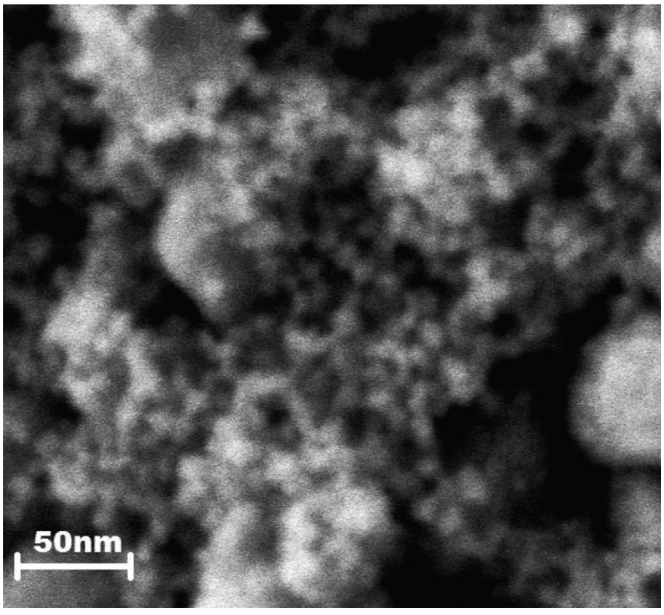

Fig. 3. FESEM micrographs of the morphology of HfO_2:Tb^{3+} NP's with 20 at% of dopant.

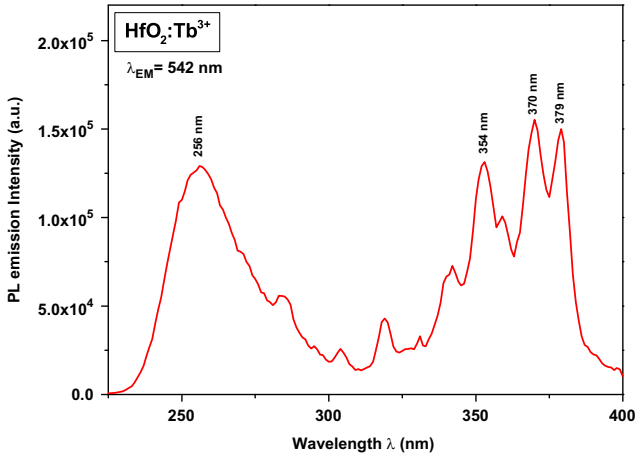

Fig. 4. Photoluminescence excitation spectrum of HfO_2 NP's with 3 at% of Tb^{3+} (λ_{EM}=542 nm).

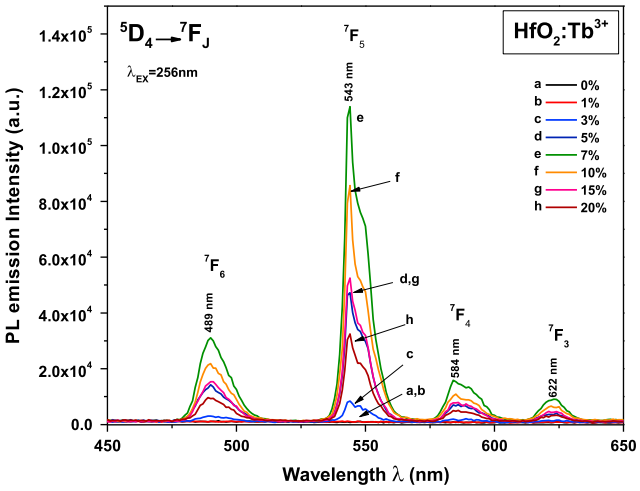

Fig. 5. Photoluminescence emission spectrums of HfO_2, at different dopant concentrations (λ_{EX}=256 nm).

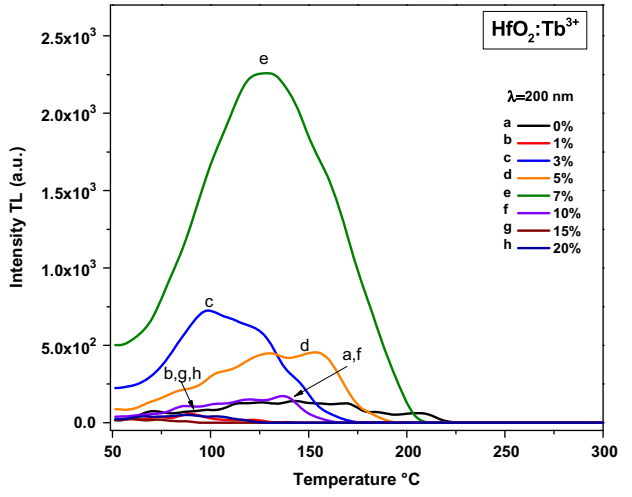

Fig. 6. TL glow curves of NPs of HfO_2:Tb^{3+}, with different dopant concentrations (λ_{UVR}=200 nm).

the NP's edges can be easily distinguished. This micrograph shows a size distribution of particles ranging from 9 to 14 nm, which is consistent with the average size obtained from the X-ray diffraction patterns.

Fig. 4 shows the photoluminescence (PL) excitation spectrum of HfO_2:Tb^{3+} with a concentration of 3 at%. The emission wavelength was set at 542 nm, which is reported as the main line of emission for terbium. It is possible to distinguish a broadband from 225 to 280 nm. This broadband whose maximum value is located at 256 nm can be ascribed to charge transfer between the matrix HfO_2 and dopant Tb^{3+} (Chacón-Roa et al., 2008). Also several peaks can be distinguished from 280 up to 390 nm.

These correspond to excitations within electronic energy levels of the Tb^{3+} ions. PL emission spectra of HfO_2:Tb^{3+} at different dopant concentrations, employing an excitation wavelength of 256 nm are shown in Fig. 5. It is possible to observe emission bands centered at 489 nm, 543 nm, 584 nm and 622 nm; associated to $^5D_4 \rightarrow {}^7F_6$, $^5D_4 \rightarrow {}^7F_5$, $^5D_4 \rightarrow {}^7F_4$, $^5D_4 \rightarrow {}^7F_3$ intra-configurational $4f \rightarrow 4f$ transitions of the Tb^{3+} ion, respectively. It is observed that the emission at 542 nm is the most intense, which gives the characteristic green color of terbium related luminescence. The maximum emission intensity is obtained at 7 at% of Tb^{3+} doping concentration. Above this concentration, the PL emission decreases as the dopant concentration increases; this can be attributed to the phenomenon of concentration quenching. This effect has been explained in terms of an increment in the migration of the excitation energy by resonant energy transfer between rare earth activators, increasing the probability to encounter a luminescent killer center (Chacón-Roa et al., 2008).

Fig. 6 exhibits the TL glow curve as a function of the dopant concentration. The TL response of the nanoparticles was measured between 50 and 300 °C, with a heating rate of 10 °C/s. A pre-heat at 50 °C was carried up before the reading. Several TL peaks are observed, of which the main peak is between 85 and 170 °C. This suggests the presence of several types of traps in the samples with different energies levels. The most intense peak in the glow curve was observed at 128 °C in the sample with Tb^{3+} 7 at%.

To determinate the order of the kinetic in the thermoluminescent process the symmetrical geometry factor μ was determined from the most intense glow curve of Fig. 6. Taking the values of $T_M = 128$ °C, $T_1 = 86$ °C and $T_2 = 172$ °C from the curve of brightness, a geometry factor $\mu = 0.5116$ was obtained, indicating that the process has a tendency to second-order kinetics where the re-entrapment of charge carriers is important. The estimated depth of the traps (activation energy) was 0.49 eV. The frequency factor "s" was determined from the activation energy, obtained a value of $s = 445{,}550\ s^{-1}$, this is an approach to determine the frequency of the trapped charge leakage. Also, this value indicates that the luminescent centers are shallow traps.

4. Conclusions

The hydrothermal synthesis technique was used to obtain luminescent nanoparticles of HfO_2 doped with Tb^{3+}. The results show that there is a relationship between dopant concentration and the degree of crystallinity of the sample; which might suggest, that the amount of Tb^{3+} ions incorporated could stabilize the tetragonal crystalline phase of hafnium oxide. Furthermore, the EDS analysis shows that there is a linear relationship of ions incorporated in the sample, depending on the amount present in the solution. The amount of oxygen, greater than the expected for HfO_2 stoichiometry, could be attributed to the presence of M–OH complexes in the samples, as suggested by the presence of the H–O absorption band in the IR spectra. The thermoluminescent characterization shows that the maximum response was obtained with a concentration of 7 at% of Tb^{3+} in the solution relative to Hf^{4+}, with an activation energy of 0.49 eV, a frequency factor $s = 445{,}550\ s^{-1}$ and a geometry factor $\mu = 0.5116$ indicating that the process has a tendency to second-order kinetics. Moreover TL analysis at different times of exposure to UVR of 200 nm, shows an increase in intensity of the glow curve, which is directly related to the amount of energy absorbed by increasing the exposure time. This behavior suggests that HfO_2:Tb^{3+} nanoparticles could be a material candidate for UVR dosimetry. The photoluminescence results show that the maximum emission occurs at a concentration of 7 at% of Tb^{3+}. This value, corresponds to the doping concentration that shows the maximum TL response, suggesting that this percentage of dopant will create the largest number of traps in the material due to the substitution of tetravalent ions (Hf^{4+}) by trivalent ions (Tb^{3+}), above this concentration, the phenomenon of concentration quenching occurs.

Acknowledgment

We thank the Consejo Nacional de Ciencia y Tecnología (CONACyT) and SIP-IPN for the financial support through the Programme nos. 20130179 and 20130101.

References

Byrappa, K., Adschiri, T., 2007. Hydrothermal technology for nanotechnology. Prog. Cryst. Growth Charact. Mater. 53 (2), 117–166.
Chacón-Roa, C., Guzmán-Mendoza, J., Aguilar-Frutis, M., García-Hipólito, M., Alvarez-Fragoso, O., Falcon, C., 2008. Characterization of luminescent samarium doped HfO_2 coatings synthesized by spray pyrolysis technique. J. Phys. D: Appl. Phys. 41, 015104–015110.
Cullity, B.D., Stock, S.R., 2001. Elements of X-Ray Diffraction. Prentice Hall, New Jersey, USA.
García-Hipólito M., 2002. Preparación mediante la técnica de rocío pirolítico y caracterización estructural, morfológica, de composición elemental y luminiscente de óxido de circonio con impurezas de tierras raras (Tb, Eu) y elementos de transición (Mn). (Tesis de Doctorado) 243 pp.
Guzmán-Mendoza, J., Aguilar Frutis, M.A., Alarcón Flores, G., García Hipólito, M., MacielCerda, A., Azorín Nieto, J., Rivera Montalvo, T., Falcony, C., 2010. Synthesis and characterization of hafnium oxide films for thermo and photoluminescence applications. Appl. Radiat. Isot. 68 (4–5), 696–699.
Lange, S., Kiisk, V., Reedo, V., Kirm, M., Aarik, J., Sildos, I., 2006. Luminescence of RE-ions in HfO_2 thin films and some possible applications. Opt. Mater. 28, 1238–1242.
LeLuyer, C., Villanueva Ibañez, M., Pillonnet, A., Dujardin, C., 2008. HfO_2:X ($X = Eu^{3+}$, Ce^{3+}, Y^{3+}) sol–gel powders for ultradense scintillating materials. J. Phys. Chem. A 112, 10152–10155.
Meskin, P.E., Yu, F., Sharikov, Ivanov V.K., Churagulov, B.R., Tretyakov, Y.D., 2007. Rapid formation of nanocrystalline HfO_2 powders from amorphous hafnium hydroxide under ultrasonically assisted hydrothermal treatment. Mater. Chem. Phys. 104 (2–3), 439–443.
Mignotte, C., 2001. EXAFS studies on erbium-doped TiO_2 and ZrO_2 sol–gel thin films. J. Non-Cryst. Solids 291, 56.
Rivera Montalvo, T., Furetta, C., Azorín Nieto, J., Falcony, C., García, M., Martínez, E., 2005. Thermoluminescence properties of high sensitive ZrO_2+PTFE for UV radiation dosimetry. Mater. Sci. Forum 480–481, 373.
Štefanić, G., Musić, S., Molčanov, K., 2005. The crystallization process of HfO_2 and ZrO_2 under hydrothermal conditions. J. Alloys Compd. 387 (1–2), 300–307.
Trüeb, R.M., Tobin, D.J., 2010. Aging Hair. Springer-Verlag, Berlin Heidelberg, pp. 113.
Villanueva-Ibañez, M., Le Luyer, C., Marty, O., Mugnier, J., 2003. Annealing and doping effects on the structure of europium-doped HfO_2 sol–gel material. Opt. Mater. 24, 51–57.
Yoshimura, M., Byrappa, K., 2008. Hydrothermal processing of materials: past, present and future. J. Mater. Sci. 43 (7), 2085–2103.
Yoshimura, M., Sōmiya, S., 1999. Hydrothermal synthesis of crystallized nanoparticles of rare earth-doped zirconia and hafnia. Mater. Chem. Phys. 61 (1), 1–8.